Mon. Not. R. Astron. Soc. **382,** 779–792 (2007) doi:10.1111/j.1365-2966.2007.12400.x

Full evolution of low-mass white dwarfs with helium and oxygen cores

J. A. Panei,[1,2]★ L. G. Althaus,[1,2]★† X. Chen[3]★ and Z. Han[3]★

[1]*Facultad de Ciencias Astronómicas y Geofísicas, UNLP, Paseo del Bosque S/N, La Plata B1900FWA, Argentina*
[2]*Instituto de Astrofísica La Plata, IALP, CONICET-UNLP*
[3]*National Astronomical Observatories/Yunnan Observatory, Chinese Academy of Sciences, Kunming 650011, China*

Accepted 2007 August 31. Received 2007 July 30; in original form 2007 January 30

ABSTRACT

We study the full evolution of low-mass white dwarfs with helium and oxygen cores. We revisit the age dichotomy observed in many white dwarf companions to millisecond pulsar on the basis of white dwarf configurations derived from binary evolution computations. We evolve 11 dwarf sequences for helium cores with final masses of 0.1604, 0.1869, 0.2026, 0.2495, 0.3056, 0.3333, 0.3515, 0.3844, 0.3986, 0.4160 and 0.4481 $M_{\odot}$. In addition, we compute the evolution of five sequences for oxygen cores with final masses of 0.3515, 0.3844, 0.3986, 0.4160 and 0.4481 $M_{\odot}$. A metallicity of $Z = 0.02$ is assumed. Gravitational settling, chemical and thermal diffusion are accounted for during the white dwarf regime. Our study reinforces the result that diffusion processes are a key ingredient in explaining the observed age and envelope dichotomy in low-mass helium-core white dwarfs, a conclusion we arrived at earlier on the basis of a simplified treatment for the binary evolution of progenitor stars. We determine the mass threshold where the age dichotomy occurs. For the oxygen white dwarf sequences, we report the occurrence of diffusion-induced, hydrogen-shell flashes, which, as in the case of their helium counterparts, strongly influence the late stages of white dwarf cooling. Finally, we present our results as a set of white dwarf mass–radius relations for helium and oxygen cores.

Key words: stars: evolution – stars: interiors – white dwarfs.

1 INTRODUCTION

It is generally accepted that most low-mass helium-core white dwarfs (He-WDs) are the result of binary star evolution, since an isolated star with low mass would take more than a Hubble time to evolve into a WD configuration. He-WDs would be the result of mass transfer episodes in close binary systems (Iben & Webbink 1989; Iben & Livio 1993). These objects have mostly been observed in various binary systems with a millisecond pulsar as companion (Edmonds et al. 2001; Bassa, van Kerkwijk & Kulkarni 2003; van Kerkwijk et al. 2005).

In addition, the existence of low-mass WDs with oxygen core (O-WD) is not discarded by theoretical calculations. In fact, Iben & Tutukov (1985) proposed several scenarios where low-mass WDs could harbour cores with elements heavier than helium. More recently, Han, Tout & Eggleton (2000) have carried out new close binary evolutionary calculations and found that some of the presumed He-WDs in double degenerate systems may actually be low-mass WDs with oxygen cores.

The presence of a WD in binary systems containing a millisecond pulsar offers an opportunity to check assumptions made about the ages of millisecond pulsar. In fact, cooling ages for WDs provide an estimation of the age of system, independent of the spin-down age of the pulsar. This is so because the pulsar spin-down begins roughly when the WD is contracting on to the cooling branch. A point to note is that low-mass WD cooling ages are strongly dependent on the thickness of the hydrogen envelope surrounding the helium core of the WD: thick hydrogen envelopes make residual hydrogen burning the main energy source of the WD. In fact, the main uncertainty weighting upon the determination of the WD cooling age is related to the thickness of the envelope.

Over the last three decades, the study of the evolution of low-mass WDs has captured the attention of researchers. Indeed, Webbink (1975) was the first to show that He-WDs develop many weak flashes as a result of thermal instabilities for masses greater than 0.17 $M_{\odot}$. As a result of residual hydrogen burning, he derived large cooling time-scales. More recently, Althaus & Benvenuto (1997) and Hansen & Phinney (1998) presented evolutionary models for low-mass He-WDs by neglecting the evolutionary history of progenitor stars. Hansen & Phinney (1998) found that thin envelopes allow the WD to cool rapidly while in WDs

★E-mail: panei@fcaglp.unlp.edu.ar (JAP); althaus@fcaglp.unlp.edu.ar (LGA); xuefeichen717@hotmail.com (XC); zhanwenhan@hotmail.com (ZH)
†Member of the Carrera del Investigador Científico y Tecnológico CONICET, Argentina.

with thick envelopes residual hydrogen burning slows down the cooling.

More recent enlightening studies by Driebe et al. (1998) and particularly Sarna, Ergma & Gerškevitš-Antipova (2000) based on an appropriate description of the evolution of progenitor stars, also predict the occurrence of several hydrogen-shell flashes before the terminal cooling branch is reached. For all of their models, including those that experience thermonuclear flashes, these authors derived thick envelopes, hence large WD cooling time-scales due to residual hydrogen burning. They could explain the evolutionary status of the binary pulsar PSR J1012+5307, in particular the large value for the spin-down age of the pulsar. Nelson, Dubeau & MacCannell (2004) also found that hydrogen burning retards the cooling process, especially for very low-mass WDs. On the other hand, they reported that if the hydrogen envelope is, somehow, completely removed (giving a naked He-WD), then the cooling times would be much shorter, as expected. They derived large cooling ages and found flashes to take place for masses in the range $0.21 \lesssim M_{\rm WD} \lesssim 0.28\,{\rm M}_{\odot}$, in good agreement with Driebe et al. (1998).

However, all of the above-mentioned results do not predict the age dichotomy suggested by observations of He-WDs companions to millisecond pulsars (see Bassa et al. 2003; Bassa 2006, and references therein). That is, WDs with stellar masses lower than about $0.18\,{\rm M}_{\odot}$ appear to evolve much more slowly than those with larger stellar masses. This age dichotomy is related to the thickness of the hydrogen envelope left in the WD (Alberts et al. 1996). In fact, WD models with thin hydrogen envelopes are required for matching the short WD cooling ages with the characteristic pulsar ages in the systems PSR J0218+4232, PSR B1855+09 and PSR J0437−4715 (see van Kerkwijk et al. 2005, for a review). Note that the mass of the WD component in these three systems is above $\approx 0.20\,{\rm M}_{\odot}$. But for PSR J1012+5307, having a very low-mass WD companion, a thick hydrogen envelope is needed to explain its old age and high effective temperature ($T_{\rm eff}$), see Bassa et al. (2006b) and Callanan, Garnavich & Koester (1998). Also a thick hydrogen envelope is expected in the ultracool low-mass WD companion to PSR J1909−3744 (see Bassa 2006). Certainly, these examples strongly suggest the existence of an age dichotomy in low-mass WDs (see Table 1).

The results presented in Althaus, Serenelli & Benvenuto (2001) and Serenelli et al. (2001) are noteworthy in this regard. In fact these authors studied the role of element diffusion in inducing thermonuclear flashes in low-mass WDs, and more importantly in explaining the envelope (and age) dichotomy required to explain the observations. It is worth mentioning that the existence of diffusion-induced hydrogen burning in DA WDs was earlier studied by Michaud & Fontaine (1984). Althaus et al. (2001) simulated the mass exchange phases by forcing the red giant branch evolution of $1\,{\rm M}_{\odot}$ model to a sufficiently large mass-loss rate, an approach also employed by Driebe et al. (1998) to obtain He-WD starting models. Althaus et al. (2001) found that for masses $M_{\rm WD} \gtrsim 0.18\,{\rm M}_{\odot}$ diffusion-induced hydrogen-shell flashes take place, which yield small hydrogen envelopes and thus a fast evolution, while He-WDs with mass less than $\approx 0.18\,{\rm M}_{\odot}$ evolve much more slowly because they retain relatively thick hydrogen envelopes. They showed that element diffusion is a key physical ingredient for matching pulsar spin-down times and WD cooling ages and thus in explaining the observed age dichotomy. We stress that thermonuclear flashes also take place in the absence of diffusion, but in this case the residual hydrogen envelope is thick enough for it not to predict an age dichotomy. The observational studies carried out by Bassa et al. (2003) are in good agreement with this theoretical prediction.

One of the aims of the present paper is to re-examine our prior conclusions about the fast evolution of low-mass WDs by recomputing the evolution of He-WDs for several masses, consistently with the expectations from close binary evolution. In addition, we study the full evolution of low-mass O-WDs, as predicted by our binary calculations. All these models were computed in a self-consistent way with the predictions of nuclear burning, time-dependent element diffusion, and the history of the WD progenitor. Our results are also presented as a set of mass–radius relations for WD models with He and O cores. The paper is organized as follows. In Section 2, we present the structure of the evolutionary codes that we have employed for computing the binary evolution and the WD evolution. In Section 3, we describe the numerical results. In Section 4, we present mass–radius relations for He- and O-WDs. Finally, in Section 5, we discuss the main implications of our results.

Table 1. WD companions to some millisecond pulsars. Listed are the WD stellar mass in solar units, the effective temperature, and the characteristic age of the pulsar $\tau_{\rm char}$ (see Bassa et al. 2003 for references, except for the labelled).

PSR	$M_{\rm WD}$ ($\rm M_{\odot}$)	$T_{\rm eff}$ (K)	$\tau_{\rm char}$ (Gyr)
J1012+5307	0.160 ± 0.020	8550 ± 25 8670 ± 300	8.9 ∓ 1.9
J0437−4715	0.236 ± 0.017	∼4750	4.9 ∓ 0.1
B1855+09	$0.258^{+0.028}_{a-0.016}$	4800 ± 800	4.9 ∓ 0.2
J0751+1807	0.16–0.21[b]	3500–4300[c]	7.1[b]
J1911−5958A	0.18 ± 0.02[d]	$10\,090 \pm 150$[d]	$2.4^{+0.9d}_{-1.0}$

[a]Kaspi, Taylor & Ryba 1994; [b]Nice et al. 2005; [c]Bassa, van Kerkwijk & Kulkarni 2006a; [d]Bassa et al. 2006b.

2 INPUT PHYSICS AND COMPUTATIONAL DETAILS

The code used in this work for binary evolution, from zero-age main-sequence (ZAMS) to pre-WD stage, is that described in Han et al. (2000), Chen & Han (2002, 2003). The code uses a self-adaptive non-Lagrangian mesh, where both the convective and semiconvective mixing are treated as a diffusion process and the simultaneous and implicit solution of both the stellar structure equations and chemical composition equations include convective mixing. It is based on an up-to-date physical description such as OPAL radiative (Rogers & Iglesias 1992) and molecular (Alexander & Ferguson 1994a,b) opacities, a detailed equation of state that includes Coulomb interactions and pressure ionization, and nuclear reaction rates from Caughlan et al. (1985) and Caughlan & Fowler (1988). Neutrino-loss rates are from Itoh et al. (1989) and Itoh et al. (1992). Convective overshooting is not considered.

For the WD regime, we employ the evolutionary code that has been used in previous works on WD evolution (Althaus et al. 2001, 2003 and references therein). Radiative opacities are those from OPAL (including carbon- and oxygen-rich compositions) for arbitrary metallicity (Iglesias & Rogers 1996). These opacities are calculated for metallicities consistent with the diffusion predictions. During the WD cooling regime gravitational settling leads to metal-depleted outer layers. In particular, the metallicity is taken as two times the abundance of CNO elements. The equation of state is an updated version of that of Magni & Mazzitelli (1979). High-density conductive opacities and the various mechanisms of neutrino emission are taken from the works of Itoh & Kohyama (1983), Itoh et al. (1983, 1984a, 1984b, 1987, 1989, 1992) and Munakata, Kohyama & Itoh (1987). Hydrogen burning is taken into account by considering

Table 2. Main characteristics of our sequences.

$M_{\rm WD}^{\rm He}$ ($M_\odot$))	$M_1^{\rm ZAMS}$ ($M_\odot$))	$q_{\rm i}$	P_0 (d)	$P_{\rm e}$ (d)
0.1869	0.50	0.45	0.20	0.7995
0.2026	0.63	0.57	0.30	1.6993
0.2495	1.26	1.14	1.03	12.384
0.3056	2.00	1.33	2.40	57.090
0.3333	2.00	1.82	2.80	85.393
0.3515	2.52	2.29	2.00	99.012
0.3844	2.52	1.68	4.00	95.388
0.3986	2.52	2.29	4.34	152.20
0.4160	2.52	2.29	5.30	165.42
0.4481	3.16	2.87	3.00	143.49
$M_{\rm WD}^{\rm CO}$ ($M_\odot$)	$M_1^{\rm ZAMS}$ ($M_\odot$)	$q_{\rm i}$	P_0 (d)	$P_{\rm e}$ (d)
0.3515	2.52	2.29	2.00	99.012
0.3844	2.52	1.68	4.00	95.388
0.3986	2.52	2.29	4.34	152.20
0.4160	2.52	2.29	5.30	165.42
0.4481	3.16	2.87	3.00	143.49

$M_{\rm WD}$: final WD mass; $= M_1^{\rm ZAMS}$: initial mass of the primary star; $q_{\rm i}$: initial mass ratio, $q_{\rm i} = M_{1,\rm ZAMS}/M_{2,\rm ZAMS}$; P_0: initial orbital period; $P_{\rm e}$: period of system at the end of binary calculations.

a complete network of thermonuclear reaction rates corresponding to the proton–proton chain and the CNO cycle. Nuclear reaction rates are taken from Caughlan & Fowler (1988).

In the present work, we take into account the evolution of the chemical abundance distribution caused by element diffusion during the whole WD stage in all of our sequences. Our treatment of time-dependent diffusion is based on the multicomponent gas treatment presented by Burgers (1969); the following nuclear species are considered: ^{1}H, ^{3}He, ^{4}He, ^{12}C, ^{14}N and ^{16}O; for more details see Althaus et al. (2001), Gautschy & Althaus (2002) and Althaus et al. (2004). Abundance changes are computed according to element diffusion and then to nuclear reactions and convective mixing. Radiative levitation, which is relevant for the distribution of surface compositions at effective temperatures greater than 30 000 K, has not been considered (see Fontaine & Michaud 1979).

In this work, we have followed the *complete* evolution of 16 WDs together with the binary evolution of their progenitors. In Table 2 we list some characteristics of the systems. Specifically, we study the evolution of 11 He-WD sequences with final masses of 0.1604, 0.1869, 0.2026, 0.2495, 0.3056, 0.3333, 0.3515, 0.3844, 0.3986, 0.4160 and 0.4481 $M_\odot$ as well as five O-WD sequences with final masses of 0.3515, 0.3844, 0.3986, 0.4160 and 0.4481 $M_\odot$. The central oxygen abundance by mass for these sequences ranges from 0.891 to 0.915. In order to derive a lower mass threshold for the occurrence of hydrogen flashes, we additionally compute the evolution for a sequence with 0.1702 $M_\odot$. This evolutive sequence was artificially obtained from 0.1604 and 0.1869 $M_\odot$ evolutive sequences both calculated from binary evolution. In particular, the initial hydrogen envelope mass for 0.1702 $M_\odot$ model, a fundamental quantity for the occurrence of flashes, was calculated by means of interpolation on the basis of realistic projections given by binary evolution. The evolutionary stages prior to the WD formation are fully accounted for by computing the conservative binary evolution of Population I progenitors. We have not taken into account the occurrence of a possible short-term Roche lobe overflow (RLOF) when the WD envelope is expanded to giant dimensions during the flashes previous to the final WD cooling branch. We started the evolution from the ZAMS through the mass transfer episodes, stages of thermonuclear flashes due to hydrogen-shell burning to the domain of WD cooling branch. For all of the sequences a solar-like initial composition (Y, Z) = (0.28, 0.02) has been adopted. The treatment of convection is that of the mixing-length theory with the ratio of the mixing length to the local pressure scaleheight set to 2 – for more details see Han et al. (2000), Chen & Han (2002, 2003). During binary evolution, we simply assume that RLOF is conservative and the calculation stops as the primary becomes a WD. In fact, the resulting WD systems will continue to evolve and result in different consequences, which depends on initial system parameters (Han, Podsiadlowski & Eggleton 1995).

For our adopted initial system parameters, our WD remnants with stellar masses larger than 0.3515 $M_\odot$ are characterized by oxygen-rich cores instead of harbouring a helium core. Indeed, in these binaries the helium core is burned in the primary star before it evolves to WD, with the consequent enrichment in oxygen and carbon (Han et al. 2000). For the sake of a direct comparison with these O-WDs, we have also calculated evolutionary sequences of He-WDs for stellar masses greater than 0.3515 $M_\odot$. To this end, we have artificially shut down the core helium burning in the whole evolutionary phase. In this way, we obtain He-WD sequences with the same stellar masses than the O-WD ones.

3 EVOLUTIONARY RESULTS

In this section we describe our main results. In Figs 1 and 2 we show the evolution in the Hertzsprung–Russell diagram (HRD) of our He-WD sequences with stellar masses of 0.1604, 0.1869, 0.2495, 0.3056, 0.3333, 0.3844, 0.3986 and 0.4481 $M_\odot$. Characteristics of the models labelled with letters along the tracks are given in Table 3 where it is listed, from left- to right-hand side, the stellar mass, the surface luminosity (in solar units), the effective temperature, the abundance by mass of surface hydrogen, the total hydrogen mass of the star (in stellar mass units), the age (in 10^6 yr) and the surface gravity. We set up time $t = 0$ after the mass-loss phase has ended. The corresponding HRDs for the O-WDs with masses of 0.3515, 0.3844, 0.3986 and 0.4481 $M_\odot$ are shown in Fig. 3 and their corresponding data are in Table 4. In Fig. 4 we show the evolution in HRD for He-WD sequence with stellar mass of 0.1702 $M_\odot$, the characteristics of which are listed in Table 5.

As is well known, hydrogen-shell burning in low-mass WDs can become unstable, leading to thermonuclear flashes by means of the CNO cycle. These flashes do not occur for WDs with masses lower $\sim$0.17 $M_\odot$ – see Webbink (1975), Driebe et al. (1998), Sarna et al. (2000) and Althaus et al. (2001). An important aspect of this and our previous studies is the role that element diffusion plays in inducing additional thermonuclear flashes. In this sense, we reinforce the conclusions arrived at in our previous studies that these additional thermonuclear flashes strongly alter the further evolution of the WD, being responsible for the presence of He-WDs with thin H envelopes. Specifically, these additional thermonuclear flashes are triggered by the tail of hydrogen distribution that is chemically diffused inwards to regions where the temperature is high enough to burn it, inducing a thermal runaway. In order to determining the threshold for the occurrence of thermonuclear flashes, we generated several sequences with masses between 0.1604 and 0.1869 $M_\odot$. We found that the threshold occurs at about 0.1702 $M_\odot$. That is, sequences with stellar masses lower than 0.1702 $M_\odot$ do not experience hydrogen flashes even in the presence of diffusion. In particular for the sequence of 0.1702 $M_\odot$, we found five flashes (see Fig. 4). The occurrence of thermonuclear flashes in most of our sequences is also in agreement with the results of previous studies that show that

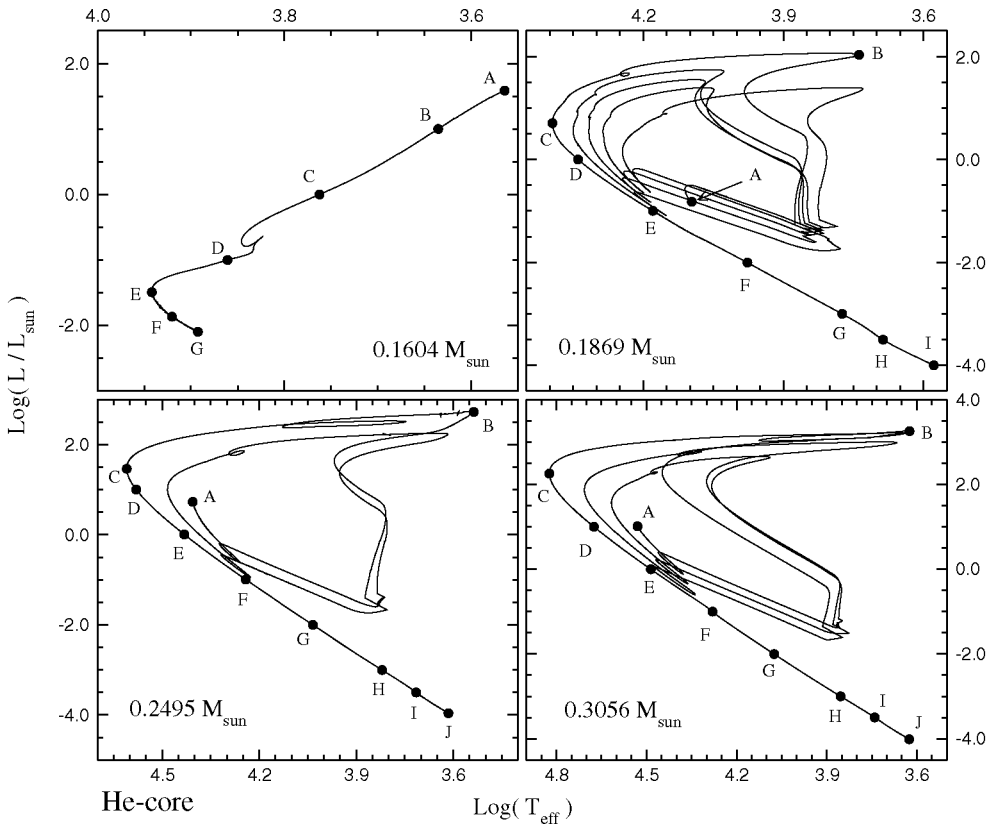

Figure 1. HRDs for He-WD evolution of 0.1604, 0.1869, 0.2495 and 0.3056 $M_\odot$. Point A denotes the end of binary evolution. The three more massive WDs experience several hydrogen-shell flash episodes before reaching the final WD cooling branch. Characteristics of the models labelled by letters are given in Table 3.

these flashes do not occur for stellar masses lower than $\sim$0.17 $M_\odot$. In addition, the occurrence of flashes in the massive sequences is in agreement with the results of Althaus et al. (2001) and are a consequence of diffusion. Indeed, for these massive WD sequences, hydrogen flashes are absent if element diffusion is not considered. This is in agreement with the predictions of other authors (who do not consider diffusion) that thermonuclear flashes do not occur for stellar masses larger than 0.25–0.30 $M_\odot$.

To better clarify the role of diffusion in the chemical evolution, we show in Figs 5–7 the inner abundance distribution of ^{1}H, ^{4}He, ^{12}C, ^{14}N and ^{16}O as a function of the outer mass fraction q ($q = 1 - m_r/M_*$). Fig. 5 corresponds to a He-WD model with 0.3333 $M_\odot$, and Figs 6 and 7, to He- and O-WD models, respectively, with a mass of 0.4481 $M_\odot$. In each figure, panel A depicts the initial chemical structure as given by binary evolution, before the model reaches the early cooling branch for the first time. Clearly, diffusion processes acting during the WD cooling track strongly modify the shape of the chemical profiles, causing hydrogen to float to the surface, and helium and heavier elements to sink down. Note the presence of a tail in the hydrogen distribution digging into deeper and hotter layers as evolution proceeds on the cooling branch. At high effective temperatures, this effect favours the occurrence of thermonuclear flashes. Note also how hydrogen goes to surface as the star evolves to the WD domain. Eventually, the pre-WD with an initially H- and He-rich envelope turns into an object with a pure hydrogen envelope (see also Tables 3 and 4). This behaviour is in sharp contrast with the results without diffusion, in which case the outer profile of chemical distribution remains constant and it is fixed by the pre-WD stage. The role of the stellar mass is also clear. For instance, from panel F note that gravitational settling has diffused heavier elements than hydrogen from the outermost $10^{-5}M_*$ of the He-WD 0.4481 $M_\odot$ model, as compared with the 0.3333 $M_\odot$ sequence at the same evolutionary stage ($L \approx 1\,L_\odot$) for which at this depth abundances have not yet changed. The behaviour for the O-WD models is qualitatively similar (compare Figs 6 and 7). In the case of the 0.4481 $M_\odot$ O-WD model, note the presence of an oxygen-rich core of about $0.82M_*$ formed during the progenitor evolution.

It is important to note that models without diffusion also experience thermonuclear flashes, but, as we mentioned, in presence of diffusion it is possible to carry hydrogen to inner and hotter regions and to induce additional flashes, which are critical for the further evolution of the star. These additional flashes will be responsible for the fact that the final hydrogen-rich envelope of the models becomes much thinner than in the case without diffusion. The reduction of the hydrogen-rich envelope after flash episodes is clear from examining Fig. 8 which depicts the evolution of the total hydrogen mass M_H (in units of $M_\odot$) versus age (in units of 10^6 yr) for 0.1604, 0.1702, 0.1869, 0.2026, 0.2495, 0.3056 and 0.3333 $M_\odot$ He-WD models. Note that because the lack of hydrogen flashes in the 0.1604 $M_\odot$ sequence, the envelope is not appreciably burnt in this case. The situation for our O-WD sequences is depicted in Fig. 9. The depicted evolutionary stages correspond to those following the end of mass transfer episodes after binary evolution. Note the hydrogen consumption that takes place after the last diffusion-induced flash episode. As a result, the hydrogen content is markedly smaller

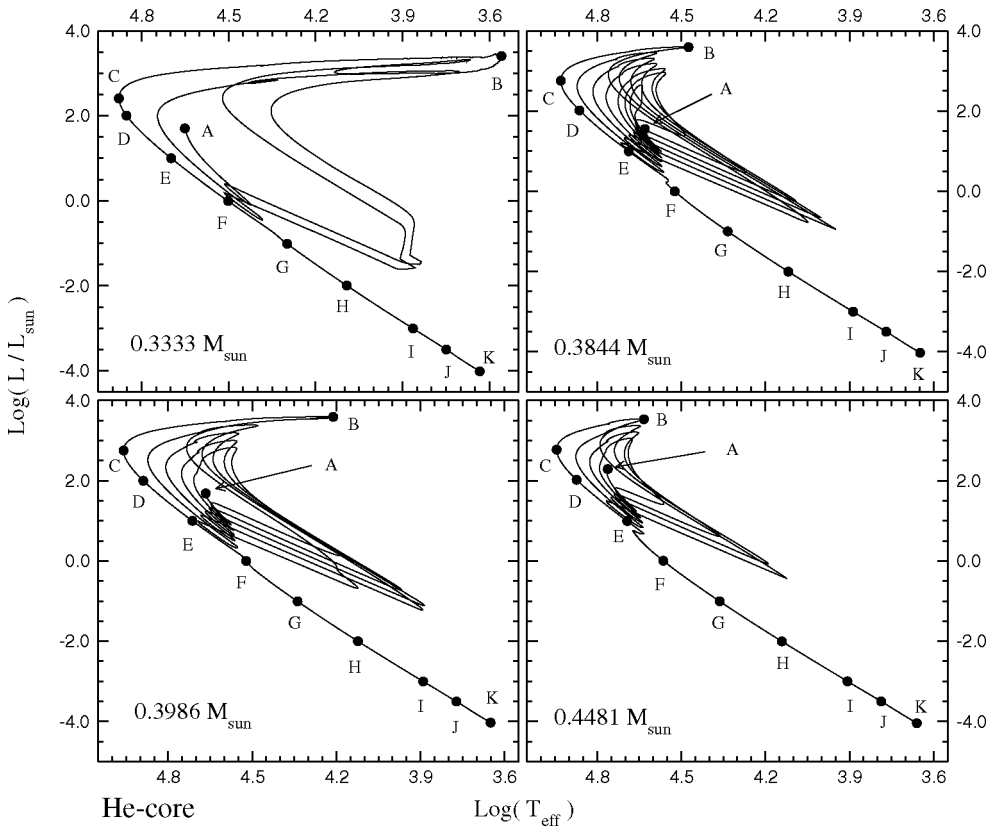

Figure 2. Same as Fig. 1 but for He-WDs with 0.3333, 0.3844, 0.3986 and 0.4481 $M_{\odot}$ sequences. Characteristics of the models labelled by letters are given in Table 3.

when the models enter the final cooling branch. Note that the most hydrogen-rich envelope is burnt in an extremely short time interval (compared with whole WD evolution) and that less massive models tend to retain a thicker hydrogen-rich envelope (this is not fulfilled for all models). For the 0.2495 $M_{\odot}$ model we include in the figure the corresponding HR track. Numbers indicate the moments when the hydrogen envelope decreases in mass during first and second thermonuclear flashes: they are the lapses 1–2 and 3–4, respectively.

Let us compare the nuclear energetics of our sequences. We stress again that all of our sequences (except for 0.1604 $M_{\odot}$ model) undergo diffusion-induced thermonuclear hydrogen flashes, giving rise to thin hydrogen envelopes. In fact, the residual hydrogen present in the WD before it enters the final cooling branch is so small that the nuclear luminosity of the object is negligible. We illustrate this in the left-hand panels of Figs 10 and 11, where the ratio of nuclear (due to proton–proton chain and CNO cycle) to photon luminosities as a function of age for He- and O-WDs is shown. Only the evolution on the final cooling branch is depicted in the figures. Note that, at advanced stages of evolution, residual hydrogen burning barely contributes to the energy budget of the WD. We conclude that diffusion prevents hydrogen burning from being a main source of energy for most of the evolution of low-mass WDs with stellar masses greater than $\approx$0.17 $M_{\odot}$. This is in contrast with the situation where diffusion is not considered, in which case residual hydrogen burning after thermonuclear flashes is the dominant energy source even at advanced stages of evolution (see Driebe et al. 1998; Althaus et al. 2001; Nelson et al. 2004). As a result, WDs obtain energy from its relic thermal content, and the cooling ages become notably smaller as compared with the case in which diffusion is neglected. The fast cooling of our sequences experiencing hydrogen flashes is documented in the right-hand panels of Figs 10 and 11, where the WD effective temperature is shown as a function of age. For two selected stellar masses, we also include with dotted lines the predictions for the 0.259 and 0.300 $M_{\odot}$ evolutionary sequences of Driebe et al. (1998). These two sequences experience thermonuclear flashes and predict ages exceedingly larger than those given by our sequences. The ages derived from the Driebe et al. (1998) sequences are in agreement with our results when diffusion is not considered in our computations (see Althaus et al. 2001). We also include in the figure the observational data for the WD companion to the millisecond pulsar PSR B1855+09 (Bassa et al. 2003). Note that our 0.2495 $M_{\odot}$ sequence is able to reproduce the very short spin-down age of PSR B1855+09, which is far from being possible if element diffusion is not considered. Our sequences are characterized by short cooling ages. This is true even for the major improvements to the treatment of the WD progenitor evolution considered in this paper, as compared with the extreme simplification for the binary evolution assumed in Althaus et al. (2001). Thus, the conclusions arrived at in Althaus et al. (2001) concerning the fast evolution resulting from the inclusion of diffusion processes appear to be robust.

As we mentioned for stellar masses lower than the mass value threshold of 0.17 $M_{\odot}$, models do not experience thermonuclear flashes even in the presence of diffusion. From our previous discussion we expect large evolutionary ages resulting from the residual nuclear burning in these low-mass WDs. This expectation is borne out in Fig. 12. Here we show the effective temperature versus age relationship for the 0.1604 $M_{\odot}$ sequence. For this sequence, the

Table 3. He-WD sequences with masses 0.1604, 0.1869, 0.2026, 0.2495, 0.3056, 0.3333, 0.3515, 0.3844, 0.3986, 0.4160 and 0.4481 $M_\odot$. Ages are counted from the end of mass transfer. We list from left- to right-hand side, the stellar mass, the luminosity (in solar units), the effective temperature, the abundance of surface hydrogen, the total hydrogen mass of the star, the age (in 10^6 yr) and the surface gravity.

He-WD		$\log(L/L_\odot)$	$\log(T_{\rm eff})$	$X_{\rm H}$	$\log(M_{\rm H}/M_*)$	Age (10^6 yr)	$\log g$ (cm s^{-2})
0.1604 $M_\odot$	A	1.5865	3.5642	0.6632	−2.1154	0.0001	1.2663
	B	1.0002	3.6353	0.6632	−2.1155	0.0026	2.1368
	C	0.0001	3.7624	0.6632	−2.1155	0.1078	3.6453
	D	−1.0002	3.8608	0.9946	−2.2053	1082.1232	5.0395
	E	−1.4927	3.9418	0.9946	−2.3641	4497.6249	5.8558
	F	−1.8649	3.9203	0.9946	−2.4901	10 000.7986	6.1420
	G	−2.0964	3.8925	0.9946	−2.5648	15 003.7337	6.2624
0.1869 $M_\odot$	A	−0.8228	4.0960	0.6632	−2.5033	0.0000	5.8692
	B	2.0323	3.7380	0.1762	−2.8887	181.1327	1.5820
	C	0.7037	4.3942	0.9900	−2.9767	183.2827	5.5354
	D	−0.0009	4.3394	0.9930	−3.0092	185.9294	6.0210
	E	−1.0003	4.1793	0.9930	−3.0116	189.4448	6.3800
	F	−2.0050	3.9770	0.9930	−3.0437	531.3227	6.5754
	G	−3.0022	3.7741	0.9930	−3.0545	1495.5746	6.7610
	H	−3.5026	3.6865	0.9920	−3.0562	2620.0375	6.9109
	I	−4.0000	3.5780	0.9919	−3.0562	4937.9009	6.9742
0.2026 $M_\odot$	A	−0.4855	4.1763	0.6475	−2.5355	0.0000	5.8883
	B	2.4053	3.6133	0.1972	−2.9395	154.1098	0.7453
	C	1.0340	4.4826	0.9656	−3.0730	155.3461	5.5941
	D	−0.0040	4.3817	0.9932	−3.1068	156.5107	6.2283
	E	−0.9971	4.2071	0.9932	−3.1080	158.6028	6.5230
	F	−2.0025	3.9990	0.9932	−3.1220	364.5618	6.6962
	G	−3.0024	3.7887	0.9932	−3.1321	1248.7294	6.8549
	H	−3.5006	3.6952	0.9930	−3.1339	2299.9990	6.9792
	I	−3.9864	3.5895	0.9930	−3.1342	4618.7451	7.0418
0.2495 $M_\odot$	A	0.7291	4.4055	0.6495	−2.7146	0.0000	5.6806
	B	2.7279	3.5367	0.3469	−2.8884	37.9214	0.2067
	C	1.4639	4.6094	0.9938	−3.1046	38.5549	5.7614
	D	1.0019	4.5803	0.9938	−3.1258	38.7383	6.1070
	E	0.0075	4.4319	0.9938	−3.1272	38.8802	6.5079
	F	−0.9939	4.2415	0.9938	−3.1281	40.8285	6.7480
	G	−2.0012	4.0342	0.9938	−3.1513	311.9422	6.9260
	H	−3.0038	3.8201	0.9938	−3.1629	1484.1152	7.0721
	I	−3.5000	3.7150	0.9938	−3.1672	2786.6130	7.1478
	J	−3.9644	3.6150	0.9938	−3.1688	5959.4206	7.2123
0.3056 $M_\odot$	A	1.0130	4.5298	0.5901	−2.8093	0.0000	5.9822
	B	3.2551	3.6245	0.2827	−3.1590	26.7389	0.1188
	C	2.2551	4.8235	0.8090	−3.4023	26.8030	5.9147
	D	1.0002	4.6752	0.9587	−3.4329	26.8378	6.5766
	E	−0.0030	4.4857	0.9940	−3.4334	26.9555	6.8216
	F	−1.0015	4.2804	0.9940	−3.4376	48.6050	6.9991
	G	−2.0031	4.0752	0.9940	−3.4706	297.6278	7.1799
	H	−2.9998	3.8537	0.9940	−3.4771	1204.7193	7.2907
	I	−3.4991	3.7401	0.9940	−3.4796	2279.2872	7.3355
	J	−4.0127	3.6258	0.9940	−3.4809	6124.5743	7.3920
0.3333 $M_\odot$	A	1.7048	4.6508	0.6244	−2.9523	0.0000	5.8120
	B	3.4069	3.5592	0.3480	−3.1781	16.8274	−0.2563
	C	2.4094	4.8781	0.8451	−3.4553	16.8716	6.0168
	D	2.0043	4.8521	0.9483	−3.4776	16.8811	6.3179
	E	1.0014	4.6976	0.9228	−3.4798	16.8913	6.7024
	F	−0.0080	4.5013	0.9333	−3.4801	17.0019	6.9270
	G	−1.0158	4.2976	0.9940	−3.4943	56.3059	7.1200
	H	−1.9968	4.0923	0.9940	−3.5237	298.4757	7.2796
	I	−3.0057	3.8645	0.9940	−3.5320	1252.1730	7.3772
	J	−3.5016	3.7497	0.9940	−3.5350	2388.6467	7.4141
	K	−4.0164	3.6339	0.9940	−3.5366	6546.9711	7.4656

Table 3 – *continued*

He-WD		$\log(L/L_\odot)$	$\log(T_{\rm eff})$	$X_{\rm H}$	$\log(M_{\rm H}/M_*)$	Age (10^6 yr)	$\log g$ (cm s^{-2})
0.3515 $M_\odot$	A	1.7603	4.4866	0.4956	−2.6499	0.0000	5.1230
	B	3.4401	4.2039	0.2518	−3.2534	13.5084	2.3124
	C	2.5424	4.8844	0.4437	−3.4242	13.5316	5.9317
	D	2.0068	4.8449	0.6241	−3.4548	13.5431	6.3096
	E	1.0015	4.6818	0.8531	−3.4578	13.5575	6.6622
	F	0.0000	4.4833	0.9940	−3.4585	13.8810	6.8697
	G	−1.0050	4.3131	0.9940	−3.5716	78.2878	7.1940
	H	−2.0083	4.0998	0.9940	−3.6008	322.6446	7.3444
	I	−2.9995	3.8738	0.9940	−3.6083	1253.9835	7.4315
	J	−3.5009	3.7567	0.9940	−3.6112	2408.2669	7.4644
	K	−4.0195	3.6390	0.9940	−3.6130	6578.1897	7.5122
0.3844 $M_\odot$	A	1.5534	4.6296	0.9945	−2.9012	3.4070	5.9407
	B	3.5921	4.4741	0.9944	−3.4109	9.2244	3.2800
	C	2.7541	4.9295	0.9944	−3.5579	9.2331	5.9395
	D	2.0158	4.8630	0.9944	−3.5853	9.2389	6.4119
	E	0.9966	4.6870	0.9944	−3.5878	9.2542	6.7272
	F	−0.0001	4.5233	0.9945	−3.6725	19.9218	7.0691
	G	−0.9986	4.3341	0.9945	−3.7731	67.0368	7.3108
	H	−2.0011	4.1182	0.9945	−3.7946	312.5599	7.4495
	I	−3.0011	3.8870	0.9945	−3.8006	1246.8674	7.5247
	J	−3.5007	3.7688	0.9944	−3.8028	2419.2594	7.5515
	K	−4.0244	3.6482	0.9942	−3.8046	6746.5220	7.5929
0.3986 $M_\odot$	A	1.6855	4.6660	0.9946	−2.8358	5.6873	5.9695
	B	3.5909	4.2115	0.3239	−3.3185	13.2418	2.2465
	C	2.7558	4.9587	0.9934	−3.5398	13.2552	6.0704
	D	2.0017	4.8885	0.9935	−3.5607	13.2593	6.5435
	E	0.9998	4.7133	0.9937	−3.5617	13.2694	6.8447
	F	0.0015	4.5219	0.9940	−3.5676	17.2673	7.0773
	G	−1.0063	4.3386	0.9940	−3.6665	70.1733	7.3521
	H	−1.9994	4.1232	0.9940	−3.6956	327.9427	7.4837
	I	−3.0018	3.8905	0.9940	−3.7050	1314.9244	7.5551
	J	−3.5015	3.7720	0.9940	−3.7084	2563.7829	7.5809
	K	−4.0307	3.6500	0.9940	−3.7105	7488.2218	7.6220
0.4160 $M_\odot$	A	1.2350	4.2123	0.5768	−1.8647	0.0000	4.6241
	B	3.6332	4.2002	0.3499	−3.3243	12.0211	2.1775
	C	2.8170	4.9811	0.9937	−3.5592	12.0331	6.1172
	D	1.9838	4.8969	0.9938	−3.5770	12.0362	6.6136
	E	1.0090	4.7229	0.9941	−3.5780	12.0465	6.8926
	F	−0.0026	4.5391	0.9941	−3.6025	19.4536	7.1690
	G	−0.9994	4.3488	0.9941	−3.6926	66.7598	7.4047
	H	−2.0033	4.1294	0.9941	−3.7242	333.6928	7.5308
	I	−3.0009	3.8965	0.9941	−3.7345	1336.0689	7.5969
	J	−3.4992	3.7779	0.9941	−3.7381	2614.9026	7.6208
	K	−4.0355	3.6536	0.9940	−3.7405	7767.3815	7.6597
0.4481 $M_\odot$	A	2.2910	4.7619	0.9378	−2.9060	4.3983	5.7988
	B	3.5320	4.6333	0.9946	−3.2339	6.6201	4.0432
	C	2.7713	4.9444	0.9946	−3.3811	6.6333	6.0485
	D	2.0220	4.8732	0.9946	−3.3979	6.6381	6.5128
	E	0.9953	4.6931	0.9946	−3.3992	6.6579	6.8190
	F	0.0058	4.5641	0.9946	−3.6253	19.7708	7.2928
	G	−1.0042	4.3630	0.9946	−3.7161	64.6371	7.4984
	H	−2.0036	4.1413	0.9946	−3.7594	345.2425	7.6109
	I	−2.9985	3.9071	0.9946	−3.7722	1387.8203	7.6693
	J	−3.4996	3.7872	0.9945	−3.7766	2751.6599	7.6905
	K	−4.0449	3.6596	0.9941	−3.7791	8360.9391	7.7257

ratio of nuclear luminosity due to proton–proton chain and CNO cycle to photon luminosity remains $\log[(L_{\rm pp} + L_{\rm CNO})/L] \approx 0$, for most of the WD evolution. That is, residual hydrogen burning is the main source of energy of star. In this figure we also include the observational predictions for PSR J1012+5037 (see Table 6). Note that in this case the large spin-down age of this pulsar is well reproduced by the WD evolutionary age.

We find that element diffusion is also a key ingredient in the evolution of low-mass O-WDs. Here, diffusion also prevents hydrogen burning from being a main energy source for most of the evolution

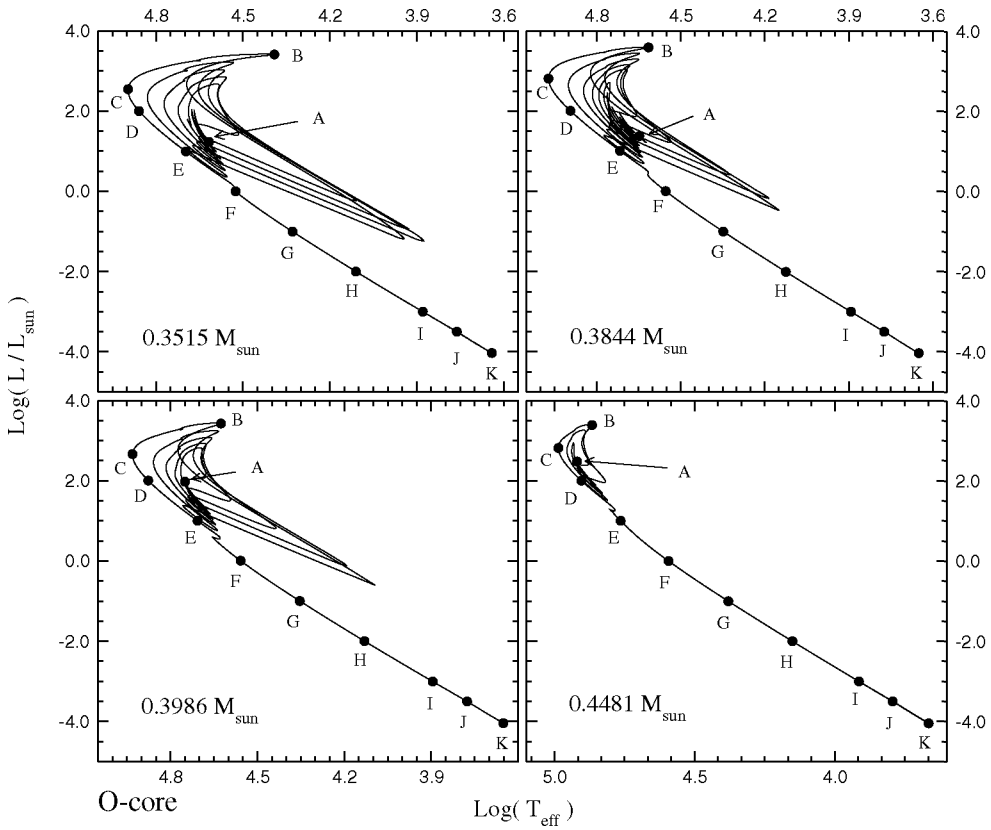

Figure 3. Same as Fig. 1 but for O-WDs with 0.3515, 0.3844, 0.3986 and 0.4481 $M_{\odot}$. Characteristics of the models labelled by letters are given in Table 4.

of these stars. As in the case of He-WDs, the O-WDs must extract energy from its relic thermal content. Thus, we expect, as compared with their He-core counterparts, low-mass O-WDs to evolve faster once they have reached their terminal cooling track. This expectation is borne out in Fig. 11 where we note that the cooling times for the O-core sequences are markedly shorter (from a factor of 0.64 – for 0.3515 $M_{\odot}$ – up to a factor of 0.45 – for 0.4481 $M_{\odot}$) than those corresponding to the He-core ones for the same stellar mass. This faster cooling is because the oxygen core is characterized by a lower total capacity of storing heat than a helium-dominated core. Another point worthy of comment is that Coulomb interactions are more relevant in the case of the O-core models. In this sense, we note that at the most advanced computing stages, all of our O-WD sequences have already started to develop a solid core.

4 MASS–RADIUS RELATIONS FOR HELIUM- AND OXYGEN-CORE WHITE DWARFS

We use the full set of stellar models calculated in this work with different masses to compute accurate mass–radius relations. We begin by examining Figs 13 and 14 where the evolution of the surface gravity is shown in terms of the $T_{\rm eff}$ for the final cooling WD branch. In Fig. 13 we add the location of some WD companions to millisecond pulsars indicated in Table 6. We also include isochrones in Myr units for 50, 100, 250, 500, 1000, 2000 and 4450. In Fig. 14 we add isochrones in Myr units for 10, 30, 100, 500, 1000 and 3700 for O-WDs.

Mass–radius relations for He-WDs are derived from the computed evolutionary sequences of 0.1604, 0.1702, 0.1869, 0.2026, 0.2495, 0.3056, 0.3333, 0.3515, 0.3844, 0.3986, 0.4160 and 0.4481 $M_{\odot}$. All of them are surrounded by a hydrogen envelope whose masses are listed in Tables 3 and 5. Mass–radius relations for He-WDs models are presented for $T_{\rm eff}$ values ranging from 4000 to 40 000 K with steps of 4000 K. For O-WDs the masses are 0.3515, 0.3844, 0.3986, 0.4160 and 0.4481 $M_{\odot}$, these models are surrounded by a helium envelope and an outermost hydrogen envelope (see Table 4). For these sequences we considered $T_{\rm eff}$ values from 5000 to 80 000 K with steps of 5000 K. For the sake of comparison, for each of the considered core compositions we have also computed the zero-temperature Hamada–Salpeter (HS) relation.

In Figs 15 and 16 we show the resulting mass–radius relations for He and O cores, respectively. In each figure, the HS zero-temperature mass–radius relations are also indicated (in Fig. 15 we depict HS homogeneous He models and in Fig. 16 HS homogeneous C models and HS homogeneous O models). As is well known, for a given stellar mass, models are characterized by larger radii at higher $T_{\rm eff}$ (Panei, Althaus & Benvenuto 2000). Note that for $T_{\rm eff} \rightarrow 0$, the radius of the models tends to the respective HS values, as expected. The behaviour exhibited by the mass–radius relations over $T_{\rm eff} \sim$ 24 000 K, in Fig. 15, is due to the hook in the evolutionary tracks caused by the re-ignition of the hydrogen shell on the terminal WD cooling branch – see also Driebe et al. (1998). These features occur at relatively short cooling ages ($<$10 Myr).

In Fig. 17 we show isothermals for He-WD models. Let us observe the break in the isothermals at lower masses. The corresponding data of observations included in figure are listed in Table 1. This figure gives evidence that WDs with masses lower than 0.17 $M_{\odot}$ have ages greater than those with masses greater than this threshold. This confirms the existence of the age dichotomy.

Table 4. Same as Table 3 but for O-WD sequences with 0.3515, 0.3844, 0.3986, 0.4160 and 0.4481 $M_\odot$.

O-WD		$\log(L/L_\odot)$	$\log(T_{\rm eff})$	$X_{\rm H}$	$\log(M_{\rm H}/M_*)$	Age (10^6 yr)	$\log g$ (cm s^{-2})
0.3515 $M_\odot$	A	1.2317	4.6170	0.4956	−2.9185	0.4959	6.1728
	B	3.4102	4.3915	0.9945	−3.3171	5.0930	3.0924
	C	2.5441	4.8962	0.9945	−3.4757	5.1118	5.9773
	D	2.0001	4.8584	0.9945	−3.4997	5.1198	6.3702
	E	0.9925	4.6967	0.9945	−3.5014	5.1309	6.7310
	F	−0.0009	4.5250	0.9945	−3.5264	11.1550	7.0377
	G	−1.0040	4.3286	0.9945	−3.6011	44.1398	7.2554
	H	−1.9990	4.1099	0.9945	−3.6211	187.9926	7.3755
	I	−3.0002	3.8791	0.9945	−3.6266	767.2916	7.4535
	J	−3.5000	3.7616	0.9942	−3.6286	1477.9360	7.4834
	K	−4.0302	3.6407	0.9940	−3.6298	4196.8893	7.5298
0.3844 $M_\odot$	A	1.3776	4.6475	0.4024	−3.0187	0.0000	6.1879
	B	3.5867	4.6150	0.9946	−3.4936	3.3220	3.8488
	C	2.8084	4.9717	0.9946	−3.6361	3.3283	6.0538
	D	2.0066	4.8935	0.9946	−3.6592	3.3320	6.5428
	E	1.0083	4.7166	0.9946	−3.6609	3.3439	6.8338
	F	0.0051	4.5533	0.9946	−3.7515	10.4537	7.1837
	G	−1.0027	4.3478	0.9946	−3.8171	37.7037	7.3698
	H	−2.0062	4.1244	0.9946	−3.8348	186.1594	7.4796
	I	−3.0009	3.8923	0.9946	−3.8386	764.2558	7.5457
	J	−3.5007	3.7734	0.9945	−3.8400	1486.1631	7.5701
	K	−4.0344	3.6498	0.9942	−3.8410	4198.1947	7.6095
0.3986 $M_\odot$	A	1.9760	4.7497	0.5528	−3.0184	1.3252	6.0142
	B	3.4272	4.6255	0.9946	−3.3111	3.1063	4.0658
	C	2.6651	4.9307	0.9946	−3.4497	3.1200	6.0490
	D	2.0058	4.8765	0.9946	−3.4690	3.1254	6.4915
	E	1.0013	4.7065	0.9946	−3.4702	3.1380	6.8158
	F	0.0075	4.5578	0.9946	−3.5889	11.0062	7.2149
	G	−0.9977	4.3533	0.9946	−3.6555	40.8114	7.4021
	H	−1.9962	4.1304	0.9946	−3.6793	199.3396	7.5093
	I	−3.0020	3.8950	0.9946	−3.6870	826.7949	7.5734
	J	−3.4997	3.7765	0.9944	−3.6896	1611.3923	7.5971
	K	−4.0400	3.6513	0.9941	−3.6912	4633.7790	7.6365
0.4160 $M_\odot$	A	2.2426	4.7879	0.5768	−3.0521	0.5670	5.9187
	B	3.4653	4.6633	0.9946	−3.3583	1.7227	4.1977
	C	2.7201	4.9556	0.9946	−3.5023	1.7336	6.1122
	D	2.0033	4.8904	0.9946	−3.5155	1.7369	6.5683
	E	0.9990	4.7170	0.9946	−3.5165	1.7514	6.8789
	F	0.0041	4.5702	0.9946	−3.6386	8.7584	7.2864
	G	−0.9944	4.3637	0.9946	−3.7013	35.2871	7.4589
	H	−2.0046	4.1362	0.9946	−3.7259	190.1781	7.5595
	I	−3.0101	3.8995	0.9946	−3.7333	793.6801	7.6181
	J	−3.5009	3.7822	0.9946	−3.7357	1539.8437	7.6396
	K	−4.0463	3.6551	0.9942	−3.7372	4582.1033	7.6765
0.4481 $M_\odot$	A	2.4799	4.9200	0.5359	−3.3348	0.1379	6.2422
	B	3.3892	4.8663	0.9732	−3.4425	0.2959	5.1180
	C	2.8176	4.9864	0.9741	−3.5182	0.3015	6.1701
	D	2.0031	4.9042	0.9748	−3.5303	0.3041	6.6558
	E	1.0014	4.7640	0.9946	−3.6145	1.1040	7.0966
	F	−0.0006	4.5930	0.9946	−3.7461	6.0284	7.4149
	G	−1.0012	4.3798	0.9946	−3.7974	26.8318	7.5628
	H	−2.0006	4.1511	0.9946	−3.8202	161.0533	7.6472
	I	−3.0000	3.9136	0.9946	−3.8267	679.1622	7.6967
	J	−3.4999	3.7933	0.9946	−3.8289	1341.8307	7.7152
	K	−4.0453	3.6647	0.9946	−3.8302	3756.9832	7.7465

5 CONCLUSIONS AND IMPLICATIONS

There is ample evidence that element diffusion is an important process that occurs in WD stars. In the field of low-mass WDs with helium cores, Althaus et al. (2001) showed that element diffusion leads to an envelope dichotomy that translates into a dichotomy in the He-WD ages. That is, for WD models with stellar masses less than about 0.17 $M_\odot$ the remnant envelope with which WDs enter their

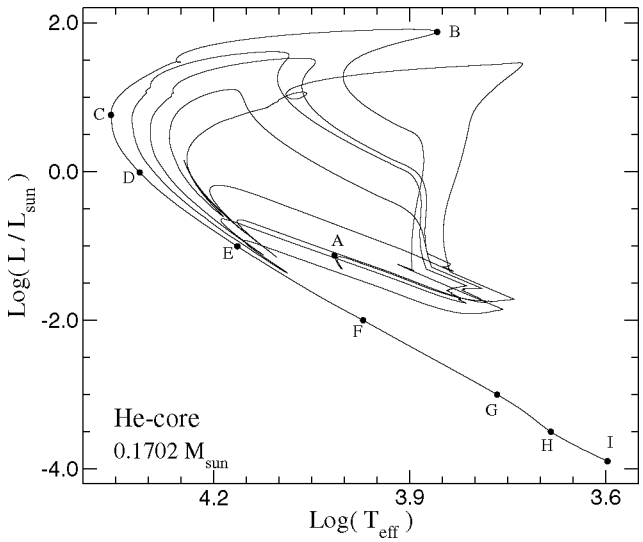

Figure 4. HRD for He-WD evolution of 0.1702 $M_\odot$. This model is the least massive one that experiences hydrogen-shell flashes. Characteristics of model labelled by letters are given in Table 5.

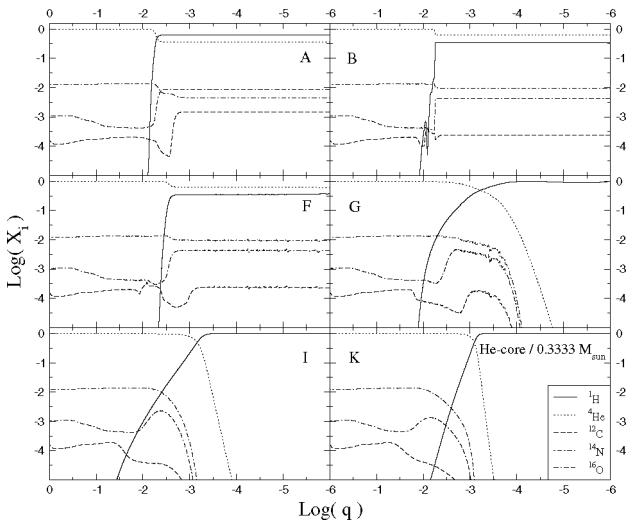

Figure 5. Abundance by mass of ^{1}H, ^{4}He, ^{12}C, ^{14}N and ^{16}O versus the outer mass fraction q ($q = 1 - m_r/M_*$) for the 0.3333 $M_\odot$ He-WD sequence at selected evolutionary stages. Labels correspond to stages shown in Fig. 2. Panel A shows the initial chemical stratification and panel B depicts the situation when model is in the red extreme in the HRD. Panels F, G, I and K depict models on the WD cooling branch. Note that diffusion alters the chemical profiles, leading to a pure hydrogen envelope and an inward diffusing hydrogen tail.

terminal cooling branch is thick enough for residual nuclear burning to yield a delay in the evolution; but for more massive WDs the envelope left is thin and evolution proceeds very fast. Specifically, element diffusion produces additional hydrogen-shell flashes, which eventually leads to very thin hydrogen envelopes. Such a dichotomy has been inferred from observational data of many WD companions to millisecond pulsars: WDs with stellar masses lower than about 0.17–0.20 $M_\odot$ appear indeed to evolve much more slowly than those with larger stellar masses (van Kerkwijk et al. 2005). As shown in Althaus et al. (2001), element diffusion appears to be a viable reason for explaining the extremely fast evolution required to match the WD age with the spin-down age of some millisecond pulsar. This is an important issue because it could constitute a clear demonstration of the existence of diffusion processes in the deep interior of WDs.

However, the study of Althaus et al. (2001) is based on simplified hypotheses about the evolution of the WD progenitor stars. Indeed in Althaus et al. (2001) the star models were obtained by simply abstracting mass from a 1 $M_\odot$ model at appropriate stages of its evolution towards the red giant branch. In this paper, we have substantially improved the treatment of the WD progenitor evolution by considering in detail the evolutionary stages leading to the formation of low-mass WDs. In particular, we have computed the full evolution of He-WDs for 11 stellar masses, consistently with the expectations from close binary evolution. The improvement in the

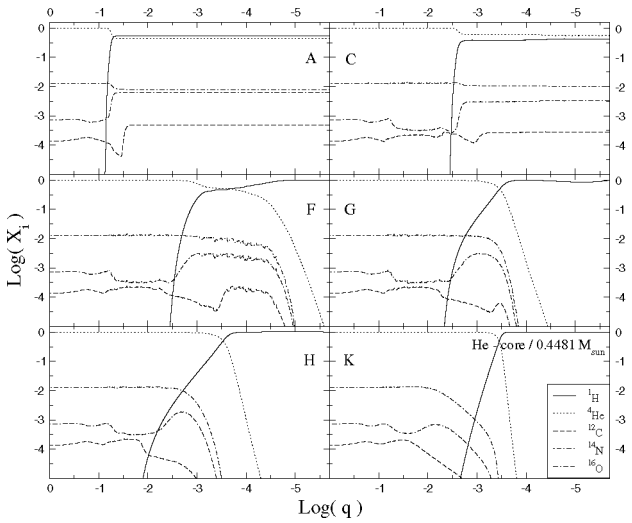

Figure 6. Same as Fig. 5 but for the 0.4481 $M_\odot$ He-WD sequence. Here, panel C corresponds to the stage when the object is in the blue extreme in the HRD. Panels F, G, H and K depict models on the WD cooling branch.

Table 5. Same as Table 3 but for He-WD sequence with 0.1702 $M_\odot$.

He-WD		$\log(L/L_\odot)$	$\log(T_{\rm eff})$	$X_{\rm H}$	$\log(M_{\rm H}/M_*)$	Age (10^6 yr)	$\log g$(cm s^{-2})
0.1702 $M_\odot$	A	−1.1274	4.0148	0.9946	−2.4717	5.7590	5.8086
	B	1.8773	3.8575	0.0869	−3.0662	853.4801	2.1745
	C	0.7599	4.3572	0.6103	−3.1068	854.2732	5.2905
	D	−0.0132	4.3131	0.9935	−3.1658	858.0296	5.8874
	E	−1.0059	4.1636	0.9935	−3.1742	862.6607	6.2823
	F	−2.0007	3.9710	0.9935	−3.1880	1041.5238	6.5064
	G	−3.0002	3.7657	0.9935	−3.2020	1965.1399	6.6849
	H	−3.4993	3.6835	0.8524	−3.1999	3041.4878	6.8552
	I	−3.8959	3.5967	0.8765	−3.1918	4491.7459	6.9044

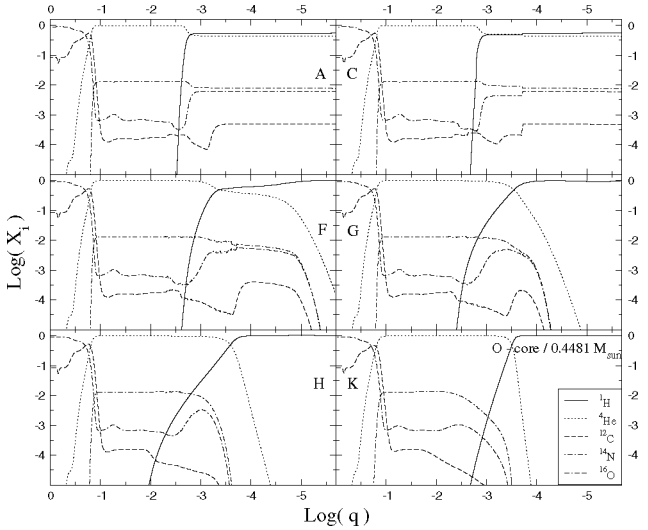

Figure 7. Same as Fig. 5 but for the 0.4481 $M_\odot$ O-WD sequence. Here, panel C corresponds to the stage when the object is in the blue extreme in the HRD. Panels F, G, H and K depict models on the WD cooling branch.

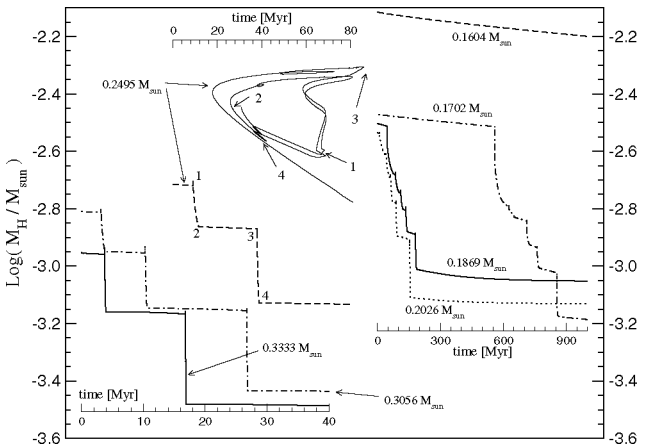

Figure 8. Total hydrogen mass M_H in solar units as a function of age for 0.1604, 0.1702, 0.1869, 0.2026, 0.2495, 0.3056 and 0.3333 $M_\odot$ He-WD models. After each flash episode, the hydrogen mass is strongly reduced as a result of nuclear burning. Thus models enter the final cooling branch with markedly small hydrogen masses. Note the extremely short time interval in which flash episode occurs. For the 0.2495 $M_\odot$ model, we include its HRD.

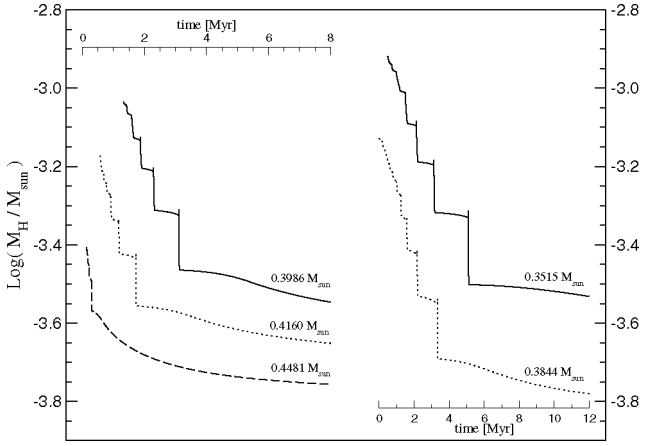

Figure 9. Same as Fig. 8 but for the 0.3515, 0.3844, 0.3986, 0.4160 and 0.4481 $M_\odot$ O-WD models.

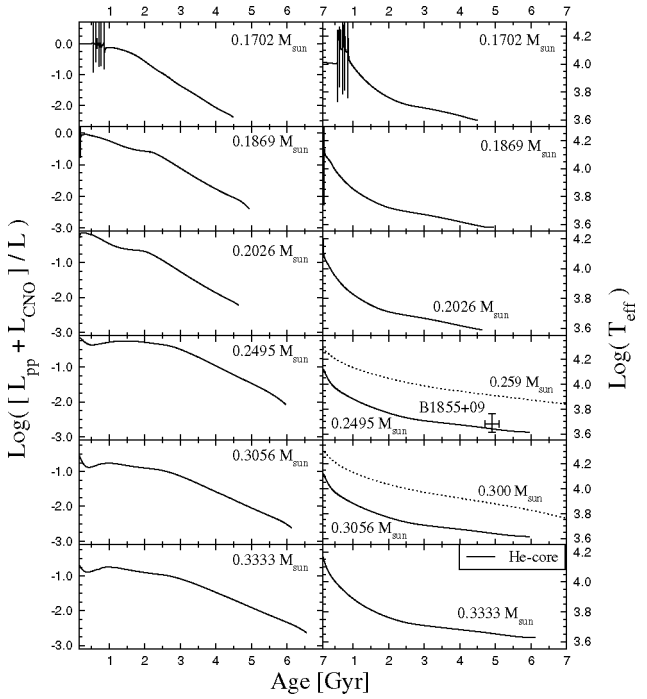

Figure 10. Ratio of nuclear (due to proton–proton chain and CNO cycle) to photon luminosities (left-hand panels) and effective temperature (right-hand panels) in terms of age for our He-WD sequences. In the interests of comparison we have included the 0.259 and 0.30 $M_\odot$ He-WD sequences of Driebe et al. (1998), denoted by dotted lines. We also include the WD companion to the millisecond pulsar PSR B1855+09.

treatment of the evolution of progenitor stars has enabled us to re-examine the conclusions arrived at in Althaus et al. (2001) about the importance of diffusion processes in low-mass WD stars.

In this paper we have not considered the possibility that processes such as meridional circulation may play a role in mitigating and even suppress the effects of diffusion-induced burning. As shown here, diffusion remains an attractive mechanism to explain the observed age dichotomy. The existence of diffusion in WDs is favoured by ample observational evidence about the occurrence of this process both in the surface layers and in the deep interior of WDs. In the case of intermediate-mass WDs, Metcalfe et al. (2005) have shown that, on the basis of asteroseismological fittings, diffusion takes place in the deep envelope of GD 358, a pulsating DB WD characterized by a stellar mass of 0.61 $M_\odot$ and a rotation velocity of 0.61 km s^{-1} (Winget et al. 1994; Kawaler 2003). Clearly, diffusion operates in the deep layers of this WD despite the presence of rotation. In low-mass WDs, we generally expect low rotation velocities. Indeed, at the beginning of RLOF, the donor corotates with the orbit, i.e. the spin period is the same as the orbital period. Since there is no known mechanism to make the spin faster during the RLOF, and if we suppose that the WD corotates with the orbit, the value of the spin period should be between the initial and final orbital periods (see P_0 and P_e in Table 2). Under this assumption, we expect He-WDs with stellar masses lower than 0.25 $M_\odot$ to rotate with velocities lower than about 0.10 km s^{-1}, i.e. much lower than the rotational velocity of GD 358. Thus, rotation would play a minor role in affecting the diffusion-induced burning in these WDs. However, for less massive

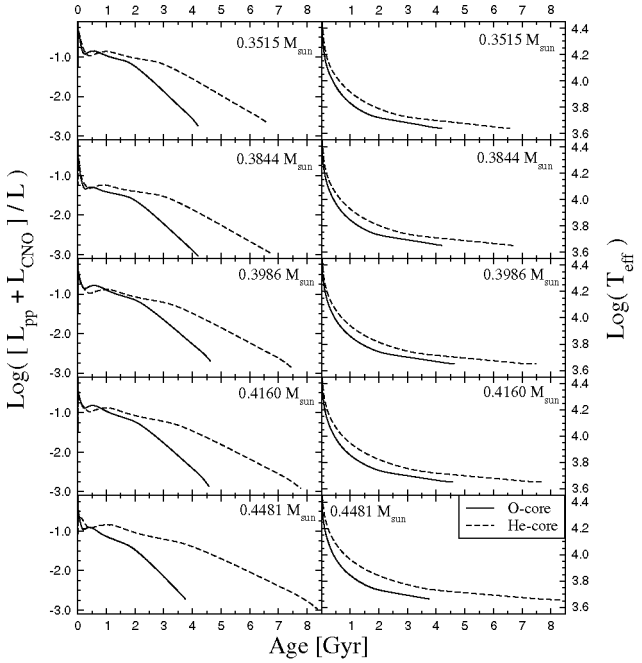

Figure 11. Same as Fig. 10 but for our He- and O-WD sequences with masses 0.3515, 0.3844, 0.3986, 0.4160 and 0.4481 $M_\odot$ (dashed and solid lines, respectively).

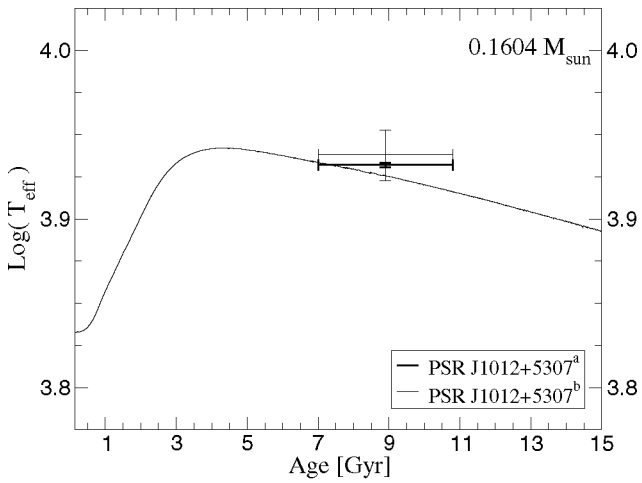

Figure 12. Effective temperature in terms of age for 0.1604 $M_\odot$ sequence. We include observational data for PSR J1012+5307 listed in Table 6.

WDs, rotational velocity becomes as high as $\approx 2\,\mathrm{km\,s^{-1}}$. For such low-mass WDs, rotation could in principle mitigate the role of diffusion in inducing thermonuclear flashes. This being the case, the mass threshold for the occurrence of thermonuclear flashes would be somewhat larger than that found here. A detailed exploration of this issue is beyond the scope of this paper and would carry us too far afield.

On the basis of these new models with realistic history, we have revisited the age of some low-mass He-WD companions to millisecond pulsars.

(i) He-WD/PSR B1855+09

This system is composed of a radio pulsar and a low-mass WD companion. The He-WD companion has a mass of $0.258^{+0.028}_{-0.016}\,M_\odot$,

Table 6. WD companions to millisecond pulsars ploted in Fig. 13. The data tabulated are the stellar mass, the effective temperature, and surface gravity.

PSR	$M_{\rm WD}$ ($M_\odot$)	$T_{\rm eff}$ (K)	$\log g(\mathrm{cm\,s^{-2}})$
J1012+5307	0.16 ± 0.02	8670 ± 300^a	6.34 ± 0.20^a
J1012+5307	0.16 ± 0.02	8550 ± 25^b	6.75 ± 0.07^b
J0751+1807	0.16–0.21^c	3500–4300^d	7.0^d
J1911−5958A	0.18 ± 0.02^e	$10\,090 \pm 150^e$	6.44 ± 0.20^e

[a]Callanan et al. (1998); [b]van Kerkwijk, Bergeron & Kulkarni (1996); [c]Nice et al. (2005); [d]Bassa et al. (2006a); [e]Bassa et al. (2006b); [f]Bassa et al. (2003).

Table 7. WD companions to millisecond pulsars plotted in Fig. 15. The data tabulated are the stellar mass and radius.

PSR	$M_{\rm WD}$ ($M_\odot$)	$R_{\rm WD}$ ($R_\odot$)
J0751+1807	0.16–0.21^a	0.021^b
J1911−5958A	0.18 ± 0.02	0.043 ± 0.009^c

[a]Nice et al. (2005); [b]Bassa et al. (2006a); [c]Bassa et al. (2006b).

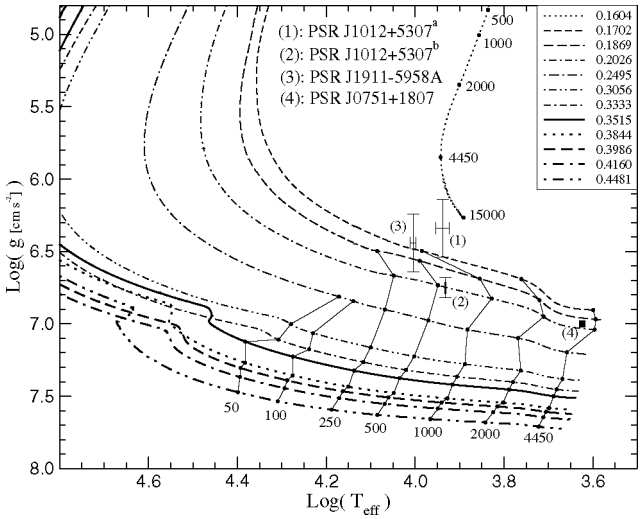

Figure 13. Surface gravity versus $T_{\rm eff}$ for 0.1604, 0.1702, 0.1869, 0.2026, 0.2495, 0.3056, 0.3333, 0.3515, 0.3844, 0.3986, 0.4160 and 0.4481 $M_\odot$ He-WD models. We plot isochrones (in Myr units) for 50, 100, 250, 500, 1000, 2000 and 4450 (segmented solid lines). We also indicate the locations of WD companions to some millisecond pulsars (see Table 6).

which has been estimated quite precisely by using the Shapiro delay of the pulsar signal – see Kaspi et al. (1994) – and a $T_{\rm eff} \approx 4800 \pm 800$ K – see Bassa et al. (2003). The characteristic age $\tau_{\rm char}$ of the pulsar is ∼5 Gyr. From our results, we found an age $\tau(0.2495\,M_\odot) \approx 3.757^{-1.514}_{+2.130}$ Gyr, in agreement with $\tau_{\rm char}$. According to the Driebe et al. (1998) evolutionary models, the WD cooling age should be ∼0 Gyr. A similar large age is also derived by Nelson et al. (2004). Driebe et al. (1998) and Nelson et al. (2004) predictions, as well as our sequences without diffusion, are at odds with the pulsar spin-down age.

(ii) He-WD/PSR J0437−4715

The He-WD companion to PSR J0437−4715 has a mass of $0.236 \pm 0.017\,M_\odot$ (from Shapiro delay) and $T_{\rm eff} \approx 4000$ K (see Bell, Bailes & Bessell 1995). From our results, we found ages $\tau(0.2026\,M_\odot) \approx 4.324$ Gyr and at $T_{\rm eff} \approx 4100$ K, $\tau(0.2495\,M_\odot) \approx 5.887$ Gyr. The characteristic age of the pulsar is ∼4.4–4.9 Gyr (Sarna et al. 2000),

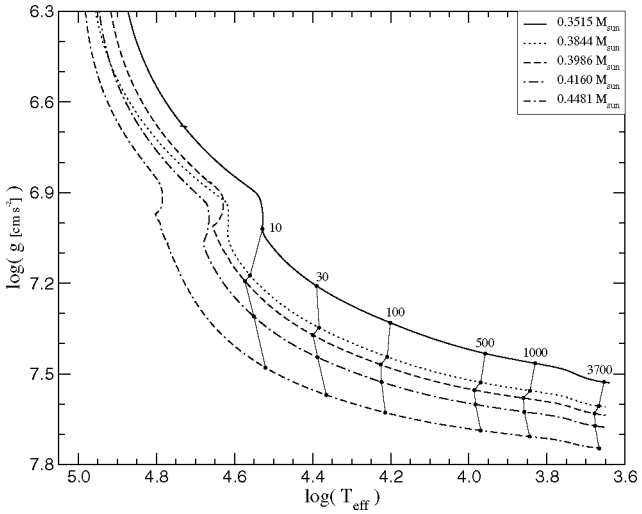

Figure 14. Same as Fig. 13 but for 0.3515, 0.3844, 0.3986, 0.4160 and 0.4481 $M_{\odot}$ O-WD models. We plot isochrones (in Myr units) for 10, 30, 100, 500, 1000 and 3700.

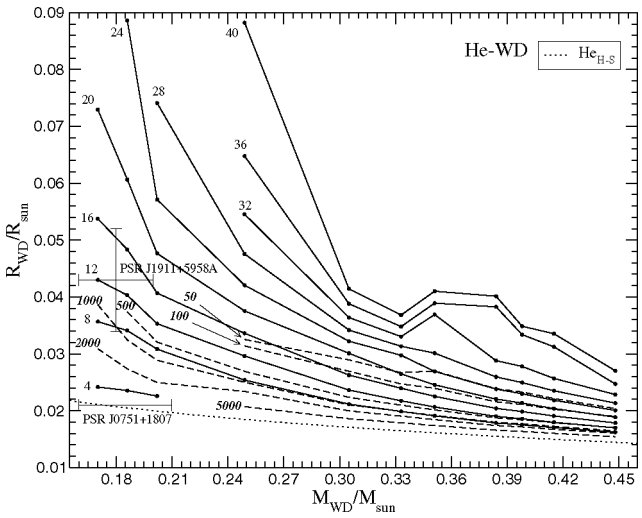

Figure 15. Mass–radius relations for He-WD models. Solid lines correspond to finite temperature models from (in 10^3 K units) 4 to 40 with steps of 4. Dotted line represents the mass–radius relation for HS homogeneous helium models. Medium dashed lines represent isochrones (in Myr units) for 50, 100, 500, 1000, 2000 and 5000.

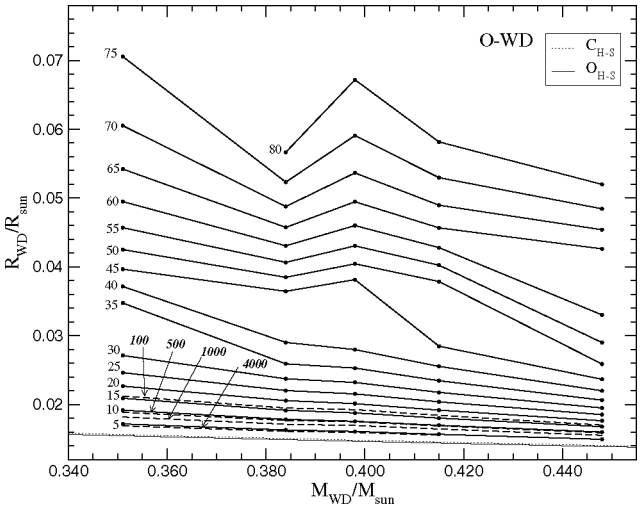

Figure 16. Mass–radius relations for O-WD models. Solid lines correspond to finite temperature models from (in 10^3 K units) 5 to 80 with steps of 5. Dotted line represents the mass–radius relation for HS homogeneous carbon models and solid thin line the HS homogeneous oxygen models. Medium dashed lines represent isochrones (in Myr units) for 100, 500, 1000 and 4000.

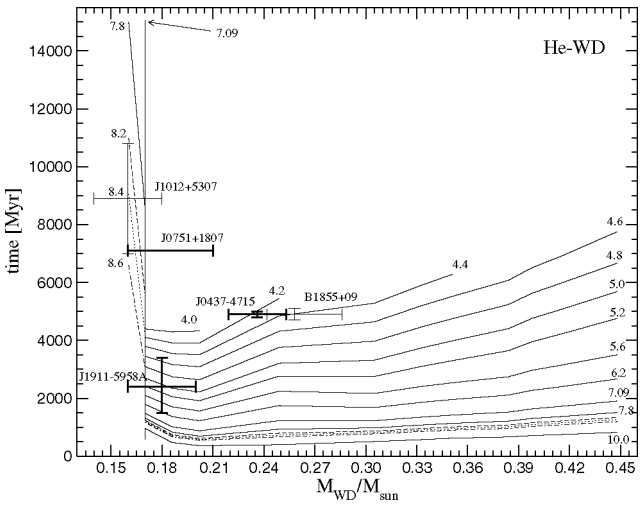

Figure 17. Isothermals for He-WD models, numbers in figure are in 10^3 K units. We also add the location of WD companions to some millisecond pulsars (see Table 1).

which is within the predictions of our models. Nelson et al. (2004) found that if the WD is about 5 Gyr its effective temperature should be higher than 8500 K, very different from the effective temperature of the WD. The models of Driebe et al. (1998) also predict for this WD ages that far exceed the characteristic age of the pulsar.

(iii) He-WD/PSR J0751+1807

The He-WD companion to the PSR J0751+1807 has a mass of $\approx$0.16–0.21 $M_{\odot}$ (Nice et al. 2005) and is a cool object, with a $T_{\rm eff} \approx$ 4300–3500 K. The characteristic age of the pulsar is $\tau_{\rm char} \sim 7.1$ Gyr (Bassa et al. 2006a). Assuming a $T_{\rm eff} \approx 3600$ K, we found an age of $\tau \approx 5.84$ Gyr (for a model of 0.2026 $M_{\odot}$). The good agreement between both ages suggests that the mass of this WD would be above the threshold value for the age dichotomy. In fact, lower stellar masses would imply ages far exceeding the spin-down age of the pulsar.

(iv) He-WD/PSR J1012+5307

The He-WD companion to this pulsar has a mass of $\approx$0.16 $\pm$ 0.02 $M_{\odot}$ (Bassa et al. 2003) and $T_{\rm eff} \approx$ 8900–8500 K. The characteristic age of the pulsar is $\tau_{\rm char} \sim 9$ Gry (Bassa et al. 2003). In this case, only WD models with thick hydrogen envelopes reproduce the large spin-down age of the pulsar.

These observational issues clearly exemplify the importance of diffusion processes in getting an agreement with the spin-down ages of some millisecond pulsars. Indeed, models with diffusion give rise to markedly smaller WD ages, as compared with the situation in which diffusion is not considered (Driebe et al. 1998; Nelson et al. 2004; and our results when diffusion is neglected: Althaus et al.

2001). The results present here reinforce the conclusions arrived at in Althaus et al. (2001) that diffusion is a key ingredient in explaining the age and envelope dichotomy observed in many WD companions of millisecond pulsar. The fast evolution above a threshold stellar mass that result from the inclusion of diffusion processes remains true even when account is made of the full binary evolution that lead to the formation of these WDs. That is the main conclusion of this work. We also determine the mass threshold for the occurrence of the age dichotomy to be about $0.17\,M_{\odot}$.

As we mentioned, the existence of diffusion processes in real stars is sustained by observational evidence. Our study suggests that the age and envelope dichotomy inferred from observations of low-mass WDs with millisecond pulsar companions could be an indication that diffusion is also a key physical ingredient in the evolution of low-mass He-WD stars.

Finally, we have assessed the evolutionary and structural properties of low-mass O-WDs with stellar masses of 0.3515, 0.3844, 0.3986, 0.4160 and $0.4481\,M_{\odot}$ as predicted by our binary calculations. For these WDs, we have reported the occurrence of diffusion-induced hydrogen-shell flashes, which, as in the case of their He-core counterparts, strongly influence the late stages of cooling. In closing, detailed mass–radius relations derived from our evolutionary sequences have been presented. We have prepared detailed tabulations for such mass–radius relations as well as for the evolutionary properties of the sequences, which are available at our web site http://www.fcaglp.unlp.edu.ar/evolgroup or upon request to panei@fcaglp.unlp.edu.ar.

ACKNOWLEDGMENTS

JAP and LGA acknowledge the Facultad de Ciencias Astronómicas y Geofísicas (UNLP) and Instituto de Astrofísica La Plata (CONICET-UNLP) for supports. We wish to thank the comments and suggestion of an anonymous referee that greatly improve the original version of this paper. We also thank Lic. H. Viturro for his technical support. This work was supported in part by the PIP 6521 grant from CONICET. XC and ZH acknowledge the support from Yunnan Natural Science Foundation (Grant 2004A0022Q) and Natural Science Foundation of China (Grants 10521001 and 10433030).

REFERENCES

Alberts F., Savonije G. J., van den Heuvel E. P. J., Pols O. R., 1996, Nat, 380, 676
Alexander D. R., Ferguson J. W., 1994a, in Jorgensen U. G., ed., Molecules in the Stellar Environment. Springer-Verlag, Berlin, p. 149
Alexander D. R., Ferguson J. W., 1994b, ApJ, 437, 879
Althaus L. G., Benvenuto O. G., 1997, ApJ, 477, 313
Althaus L. G., Serenelli A. M., Benvenuto O. G., 2001, MNRAS, 323, 471
Althaus L. G., Serenelli A. M., Córsico A. H., Montgomery M. H., 2003, A&A, 404, 593
Althaus L. G., Córsico A. H., Gautschy A., Han Z., Serenelli A. M., Panei J. A., 2004, MNRAS, 347, 125
Bassa C. G., 2006, PhD thesis, Universiteit Utrecht
Bassa C. G., van Kerkwijk M. H., Kulkarni S. R., 2003, A&A, 403, 1067
Bassa C. G., van Kerkwijk M. H., Kulkarni S. R., 2006a, A&A, 450, 295
Bassa C. G., van Kerkwijk M. H., Koester D., Verbunt F., 2006b, A&A, 456, 295
Bell J. F., Bailes M., Bessell M. S., 1995, Nat, 364, 603
Burgers J. M., 1969, Flow Equations for Composite Gases. Academic Press, New York
Callanan P. J., Garnavich P. M., Koester D., 1998, MNRAS, 298, 207
Caughlan G. R., Fowler W. A., 1988, At. Data Nucl. Data Tables, 40, 284
Caughlan G. R., Fowler W. A., Harris M. J., Zimmerman B. A., 1985, At. Data Nucl. Data Tables, 35, 198
Chen X., Han Z., 2002, MNRAS, 335, 948
Chen X., Han Z., 2003, MNRAS, 341, 662
Driebe T., Schönberner D., Blöcker T., Herwig F., 1998, A&A, 339, 123
Edmonds P. D., Gilliland R. L., Heinke C. O., Grindlay J. E., Camilo F., 2001, ApJ, 557, L57
Fontaine G., Michaud G., 1979, ApJ, 231, 826
Gautschy A., Althaus L. G., 2002, A&A, 382, 141
Han Z., Podsiadlowski P., Eggleton P. P., 1995, MNRAS, 272, 800
Han Z., Tout C. A., Eggleton P. P., 2000, MNRAS, 319, 215
Hansen B. M. S., Phinney E. S., 1998, MNRAS, 294, 557
Iben I. Jr., Livio R. F., 1993, PASP, 105, 1373
Iben I. Jr., Tutukov A. V., 1985, ApJ, 58, 661
Iben I. Jr., Webbink R. F., 1989, in Wegner G., ed., Proc. IAU Colloq. 114, White Dwarfs. Springer-Verlag, Berlin, p. 477
Iglesias C. A., Rogers F. J., 1996, ApJ, 464, 943
Itoh N., Kohyama Y., 1983, ApJ, 275, 854
Itoh N., Mitake S., Iyetomi H., Ichimaru S., 1983, ApJ, 273, 774
Itoh N., Kohyama Y., Matsumoto N., Seki M., 1984a, ApJ, 285, 304
Itoh N., Kohyama Y., Matsumoto N., Seki M., 1984b, ApJ, 285, 758
Itoh N., Kohyama Y., Matsumoto N., Seki M., 1987, ApJ, 322, 584 (erratum)
Itoh N., Adachi T., Nakagawa M., Kohyama Y., Munakata H., 1989, ApJ, 339, 354 (erratum: 1990, ApJ, 360, 741)
Itoh N., Mutoh H., Hikita A., Kohyama Y., 1992, ApJ, 395, 622 (erratum: 1993, ApJ, 404, 418)
Kaspi V. M., Taylor J. H., Ryba M. F., 1994, ApJ, 428, 713
Kawaler S. D., 2003, Proc. IAU Symp. 215, in Maeder A., Eenens P., eds, Stellar Rotation. Astron. Soc. Pac., San Francisco, p. 561
Magni G., Mazzitelli I., 1979, A&A, 72, 134
Metcalfe T. S., Nather R. E., Watson T. K., Kim S.-L., Park B.-G., Handler G., 2005, A&A, 435, 649
Michaud G., Fontaine G., 1984, ApJ, 283, 787
Munakata H., Kohyama Y., Itoh N., 1987, ApJ, 316, 708
Nelson L. A., Dubeau E., MacCannell K. A., 2004, ApJ, 616, 1124
Nice D. J., Splaver E. M., Stairs I. H., Löhmer O, Jessner A., Kramer M., Cordes J. M., 2005, ApJ, 634, 1242
Panei J. A., Althaus L. G., Benvenuto O. G., 2000, A&A, 353, 970
Rogers F. J., Iglesias C. A., 1992, ApJS, 79, 507
Sarna M., Ergma E., Gerškevitš-Antipova J., 2000, MNRAS, 316, 84
Serenelli A. M., Althaus L. G., Rohrmann R. D., Benvenuto O. G., 2001, MNRAS, 325, 607
van Kerkwijk M. H., Bergeron P., Kulkarni S. R., 1996, ApJ, 467, L89
van Kerkwijk M. H., Bassa C. G., Jacoby B. A., Jonker P. G., 2005, in Rasio F. A., Stairs I. H., eds, ASP Conf. Ser. Vol. 328, Binary Radio Pulsars. Astron. Soc. Pac., San Francisco, p. 357
Webbink R. F., 1975, MNRAS, 171, 555
Winget D. E. et al., 1994, ApJ, 430, 839

This paper has been typeset from a TEX/LATEX file prepared by the author.